Journal of Solid State Chemistry 182 (2009) 3211–3214

Contents lists available at ScienceDirect

Journal of Solid State Chemistry

journal homepage: www.elsevier.com/locate/jssc

Rapid Communication

Three-dimensional (3-D) metal-organic frameworks with 3-pyridin-4-yl-benzoate defining new (3,6)-connected net topologies

Xiu-Juan Jiang [a,b], Miao Du [a,b,*], Yan Sun [a], Jian-Hua Guo [a], Jin-Shan Li [b,**]

[a] College of Chemistry and Life Science, Tianjin Key Laboratory of Structure and Performance for Functional Molecule, Tianjin Normal University, Tianjin 300387, PR China
[b] State Key Laboratory of Elemento-Organic Chemistry, Nankai University, Tianjin 300071, PR China

ARTICLE INFO

Article history:
Received 1 July 2009
Received in revised form
2 September 2009
Accepted 7 September 2009
Available online 11 September 2009

Keywords:
Metal-organic frameworks
Network topology
Mixed connectivity
Thermal stability
Fluorescence

ABSTRACT

Reactions of different metal salts with 3-pyridin-4-yl-benzoic acid (3,4-Hpybz) under ambient condition afford a series of 3-D metal-organic frameworks with two new types of (3,6)-connected net topologies. In the isomorphic complexes $[M_2(\mu\text{-}H_2O)(3,4\text{-pybz})_4]_n$ (M^{II}=Mn^{II} for **1**, Zn^{II} for **2**, or Cd^{II} for **3**), the octahedral metal nodes are extended by the 3-connected pybz tectons to constitute 3-D arrays with the Schläfli symbol of $(3.4.5)(3^2.4^4.5^5.6^2.7^2)$, whereas $[Pb(3,4\text{-pybz})_2]_n$ (**4**) shows a completely different 3-D $(4^2.6)_2(4^4.6^2.8^9)$ framework, which represents a subnet of the (4,8)-connected fluorite lattice.

Research in the area of metal-organic frameworks (MOFs) continues to be interesting in recent years for their fascinating topological architectures and useful properties [1–4]. In fact, a profound understanding of the topology issue of high-dimensional MOFs represents one of the most important subjects, because it will radically accelerate the discovery of new MOFs materials with specific functions [5]. Thus, network topology of such crystalline solids containing the required geometry information and binding fashion of the building components, is an essential topic for designing MOFs, and by using this approach, the complicated structures can be simplified to node-and-connection nets [5]. On the other hand, a majority of typical 3-D MOFs can be regarded as the prototypes of natural metallic or binary inorganic materials (such as α-Po, NbO, Pt_3O_4, Cd_SO_4, PtS, CaB_2, $SrSi_2$, diamond, feldspar, boracite, perovskite, pyrite, quartz, rutile, sodalite, fluorite, anatase, tungsten bronze, and zeolite, etc.), which will undoubtedly expand the possible applications for such crystalline materials [5,6]. It is well known that networks with 3-, 4-, or 6-connectivity are of most relevance, and multifarious such uninodal coordination frameworks have been realized [5,7–9]. However, high-dimensional nets with mixed connectivity, such as (3,6)-, (4,6)-, and (4,8)-connected architectures, are still quite rare [6,10,11] and more work is required to focus on this subject.

Recently, several efforts have been made to explore the coordination chemistry of pyridylcarboxylate derivatives such as 3-pyridin-3-yl-benzoate (3,3-pybz) and 4-pyridin-4-yl-benzoate (4,4-pybz), which can afford a variety of 1-D, 2-D, and 3-D coordination polymers with different metal ions [12]. However, their isomeric building block 3-pyridin-4-yl-benzoate (3,4-pybz, see Chart 1) has not been concerned so far. Herein, we will present a series of 3-D MOFs (**1**–**4**) assembled from Mn^{II}, Zn^{II}, Cd^{II}, or Pb^{II} with 3,4-Hpybz, and demonstrate its significant potential for constructing interesting coordination frameworks with new (3,6)-connected topologies.

Complexes **1**–**4** were synthesized by the direct reactions of 3,4-Hpybz with different metal salts in DMF/CH_3OH solution, and X-ray quality single crystals were obtained by slow solvent evaporation [13]. The composition of all products was confirmed by elemental analyses and IR spectra, and their phase purity of the bulk samples was identified by powder X-ray diffraction (PXRD) patterns (see Fig. S1). For the IR spectra of **1**–**3**, the broad bands centered at ca. 3400 cm^{-1} indicate the O–H stretching of water. Notably, in the IR spectra of **1**–**4**, the absence of characteristic absorption bands of the carboxyl group reveals the complete deprotonation of the ligand. As a consequence, the antisymmetric and symmetric stretching vibrations of carboxylate are observed in the range of 1594–1626 and 1353–1398 cm^{-1}, respectively.

All complexes are air stable and their thermal stability was explored by thermogravimetric and differential thermal analysis (TG-DTA) technique (see Fig. S2). The TG curves of **1**–**3** are similar,

---

* Corresponding author at: College of Chemistry and Life Science, Tianjin Key Laboratory of Structure and Performance for Functional Molecule, Tianjin Normal University, Tianjin 300387, PR China. Fax: +86 22 2376 6556.

** Corresponding author.

E-mail addresses: dumiao@public.tpt.tj.cn (M. Du), jinshanl@nankai.edu.cn (J.-S. Li).

0022-4596/$ - see front matter © 2009 Elsevier Inc. All rights reserved.
doi:10.1016/j.jssc.2009.09.004

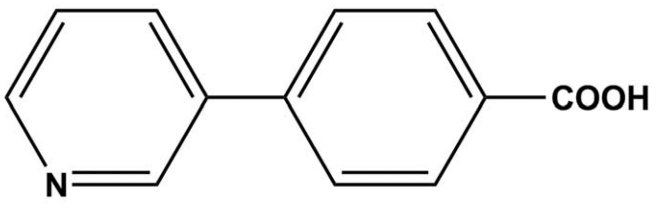

Chart 1. Schematic representation of the ligand 3,4-Hpybz.

probably due to their isostructural nature. The coordination framework is thermally stable to ca. 360 °C, beyond which a sharp weight loss occurs and stops at ca. 520 °C. Accordingly, two intensive exothermic peaks are observed at 420 and 446 °C in the DTA curve for **1** (one weak endothermic peak at 394 °C plus two intensive exothermic peaks at 428 and 491 °C for **2**, and two intensive exothermic peaks at 402 and 440 °C for **3**). These results clearly reveal the robust complexation of the water entity due to its strong bridging coordination fashion. Pyrolysis of complex **4** is observed until heating to 293 °C and the corresponding sharp weight loss ends at 472 °C. Accordingly, one weak endothermic peak at 414 °C and one intense exothermic peak at 456 °C are observed in the DTA curve.

Solid-state luminescent properties of the Zn$^{\text{II}}$, Cd$^{\text{II}}$, and Pb$^{\text{II}}$ complexes **2**–**4** were investigated at room temperature (see Fig. S3). Excitation of the microcrystalline samples of **2**–**4** results in similar fluorescent emissions with the peak maxima occurring at 376 nm for **2** (λ_{ex}=326 nm), 390 nm for **3** (λ_{ex}=332 nm), and 361 nm for **4** (λ_{ex}=327 nm), respectively. Additionally, the fluorescent spectrum of the free ligand 3,4-Hpybz displays the maximum emission peak at 387 nm (λ_{ex}=327 nm, see Fig. S3). These results indicate that the maximal emissions of complexes **2**–**4** should originate from the ligand-centered transitions. Notably, the fluorescent intensity of **4** is significantly weaker than that of the ligand and other complexes, and the quenching of fluorescence in this case may be attributed to the heavy atom effect of the Pb$^{\text{II}}$ ion [4a].

Single crystal X-ray diffraction analysis [14] suggests that complexes **1**–**3** are isomorphic, and thus, only the crystal structure of **1** is described here. The asymmetric unit of **1** consists of one Mn$^{\text{II}}$ ion, two 3,4-pybz anions, and one water ligand with two-fold symmetry. Each six-coordinated Mn$^{\text{II}}$ center is surrounded by two pyridyl nitrogen donors and three carboxylate oxygen atoms coming from different 3,4-pybz ligands as well as one oxygen atom from the water molecule, taking a distorted octahedral geometry (see Fig. 1a). In this structure, the carboxylate group in one 3,4-pybz ligand adopts the *syn*,*syn*-bridging coordination mode, whereas that in the other is unidentate. Both independent 3,4-pybz tectons are also bound to the metal ions via the pyridyl nitrogen donors thereof. In virtue of the bridging roles of carboxylate and ligated water entities, two adjacent Mn$^{\text{II}}$ centers are combined to constitute a [$Mn_2(\mu\text{-}H_2O)(COO^-)_2$] dinuclear unit (see Fig. 1a) with the Mn···Mn separation of 3.749(2) Å. In addition, each water component is also hydrogen bonded to a pair of uncoordinated carboxylate oxygen atoms around it [O5···O3 and H5···O3 distances=2.592 and 1.76 Å; O5–H5···O3 angle=166°], which may further stabilize this dinuclear pattern. As a consequence, such dimeric subunits are extended by the ligand backbones to afford a 3-D coordination framework (see Fig. S4).

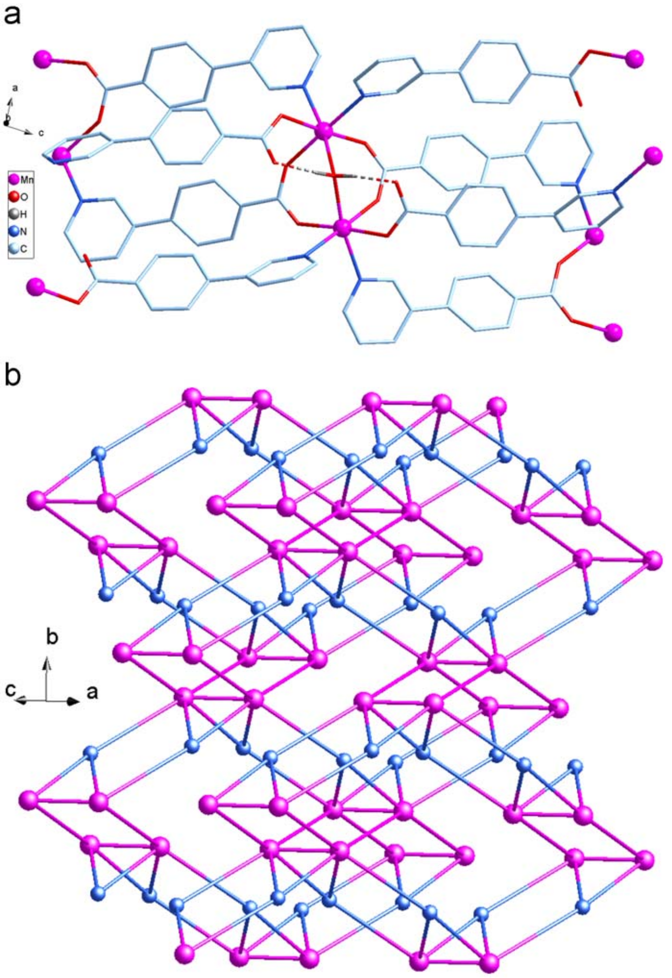

Fig. 1. Views of **1**. (a) Local coordination environment of Mn$^{\text{II}}$. The hydrogen bonds in the dimeric unit are shown as dashed lines. (b) Schematic view of the (3,6)-connected network (blue nodes for the 3-connected 3,4-pybz ligands and pink ones for the Mn$^{\text{II}}$ ions). (For interpretation of the references to color in this figure legend, the reader is referred to the webversion of this article.)

From the perspective of net topology, the two types of 3,4-pybz ligands in this 3-D structure serve as the two-connected spacer and three-connected node, respectively, and each Mn$^{\text{II}}$ center acts as a six-connected node, linking to three 3-connected 3,4-pybz tectons plus three adjacent Mn$^{\text{II}}$ ions via the 3,4-pybz spacers. Thus, a binodal (3,6)-connected network with the Schläfli symbol of $(3.4.5)(3^2.4^4.5^5.6^2.7^2)$ is constituted (see Fig. 1b). On the other hand, if we consider the dimeric motifs stated above as the secondary building units (SBUs), this 3-D network can also be simplified to a uninodal 4-connected diamond topology (see Fig. S5).

In comparison with 3,4-pybz, its isomer 3,3-pybz can adopt the *cis*- or *trans*-conformation to meet the steric requirement upon metal complexation. As for the Zn$^{\text{II}}$ and Cd$^{\text{II}}$ complexes of 3,3-pybz, they display the 1-D double-strand helical array and 3-D coordination network with unusual (3,5)-connectivity, respectively [12b]. However, with respect to the 4,4-pybz ligand, it serves as a linear linker in the coordination networks of its Zn$^{\text{II}}$ and Cd$^{\text{II}}$ complexes, resulting in the familiar diamondoid structures of 5- and 7-fold interpenetration [12c]. Their structural discrepancy may mainly originate from the significant isomeric effect of the pybz building blocks.

Divalent lead ion bears large cationic radius and identifiable void for the disposition of organic ligands, which can be termed as "inert-pair effect" [15]. Previous studies have indicated that the stable and relatively inert outer lone pair of electrons around Pb$^{\text{II}}$ can result in a nonspherical charge distribution, responsible for the unusual coordination features of Pb$^{\text{II}}$ with a wide range of coordination numbers and irregular geometries [16,17]. In this work, the Pb$^{\text{II}}$ complex **4** also displays a (3,6)-connected coordination network, which however is completely different to that of **1**–**3** [14]. The asymmetric unit of **4** contains one Pb^{II} ion that lies on a point of 2/n symmetry and one 3,4-pybz ligand. Each Pb^{II} center is eight-coordinated to six carboxylate oxygen atoms and two pyridyl nitrogen donors coming from six separated 3,4-pybz ligands (see Fig. 2a). As a result, the Pb^{II} centers are interconnected by the 3,4-pybz modules to furnish a compact 3-D coordination framework (see Fig. S6). In this architecture, each 3,4-pybz is linked to three Pb^{II} ions via one pyridyl nitrogen and the bridging carboxylate group, whereas each Pb^{II} center is coordinated to six 3,4-pybz anions. Thus, from the standpoint of network topology, each 3,4-pybz represents a 3-connected node to combine with the 6-connected Pb^{II} ions, generating a 3-D (3,6)-connected network with the Schläfli symbol of $(4^2.6)_2(4^4.6^2.8^9)$ (see Fig. 2b).

Our recent report has summarized the known 3-D architectures with (3,6)-connectivity observed in both MOFs [such as rutile (**rtl**), pyrite (**pyr**), and anatase (**ant**)] and inorganic materials [including α-PbO_2 (**apo**), ramsdellite (γ-MnO_2), brookite (**brk**), and PrI_2 (**spn**)] [10c,18]. As far as we know, the network structures of **1**–**4** indicate the unprecedented 3-D (3,6)-connected topologies. Notably, a further structural analysis of **4** reveals that it represents a subnet of the fluorite (**flu**) topology with (4,8)-connectivity. A topological calculation by using the TOPOS software suggests that such a network is derived from **flu** by decreasing its space-group symmetry from $Fm\overline{3}m$ to $Pccn$, with shifting the origin by (1/4, 0, 1/4) vector and breaking quarter of the connecting bonds (see Fig. 3) [19,20].

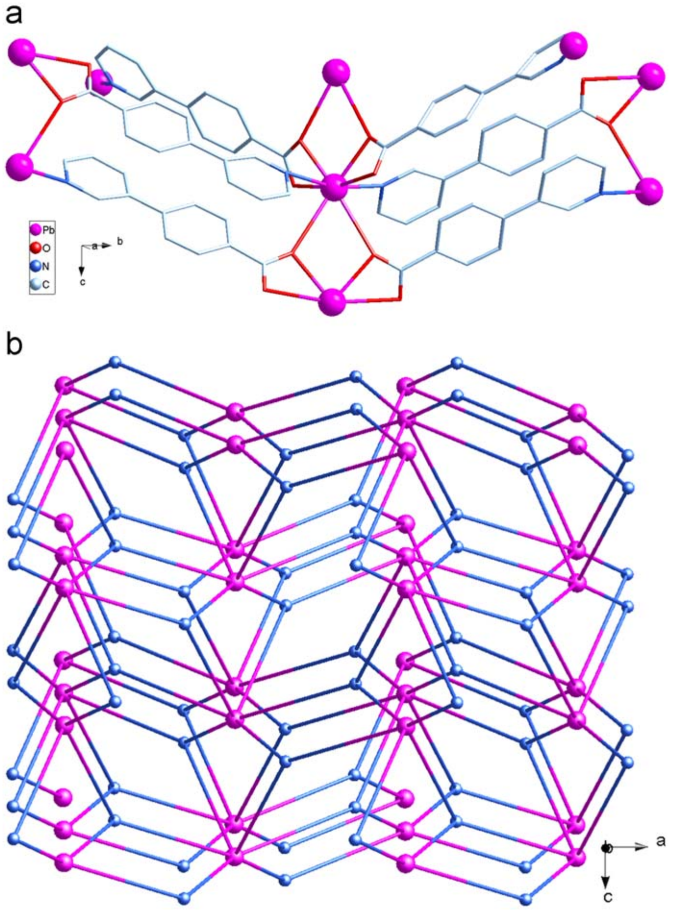

Fig. 2. Views of **4**. (a) Local coordination environment of Pb^{II}. (b) Schematic view of the (3,6)-connected network (blue nodes for the 3-connected 3,4-pybz ligands and pink ones for the Pb^{II} ions). (For interpretation of the references to color in this figure legend, the reader is referred to the webversion of this article.)

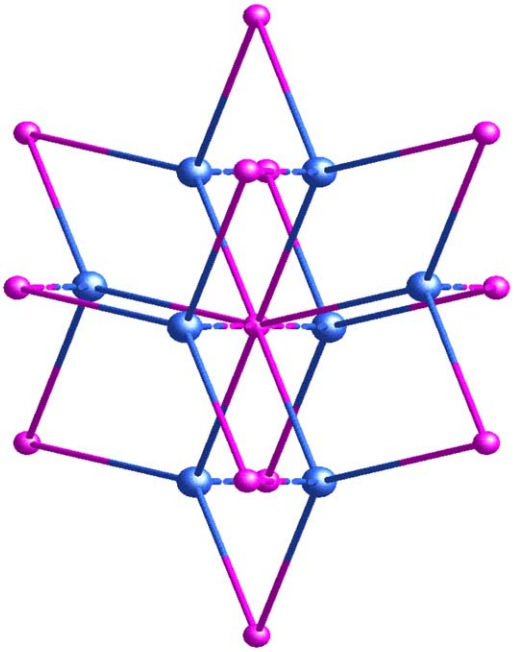

Fig. 3. Schematic view of obtaining the (3,6)-connected net of **4** from the (4,8)-connected **flu** topology by removing 1/4 of the bonds (indicated as dashed lines).

In conclusion, assembling the rigid building block 3-pyridin-4-yl-benzoic acid with the familiar metal ions such as Mn^{II}, Zn^{II}, Cd^{II}, or Pb^{II} leads to the formation of four unique 3-D MOFs with new (3,6)-connected network topologies, which will significantly enrich the relevant knowledge of crystal engineering for coordination solids. This work also reveals that such an anionic tecton may potentially act as an effective connector for the design and construction of mixed-connected coordination frameworks and further efforts on this perspective are underway.

This work was financially supported by the National Natural Science Foundation of China (20671071), Program for New Century Excellent Talents in University (NCET-07-0613), Tianjin Normal University, and SRF for ROCS, SEM. We also thank Professors M. O'Keeffe and V.A. Blatov for their invaluable comments on network topology.

Appendix A. Supplementary material

Supplementary data associated with this article can be found in the online version at doi:10.1016/j.jssc.2009.09.004.

References

[1] (a) C. Janiak, Dalton Trans. (2003) 2781;
(b) O.M. Yaghi, M. O'Keeffe, N.W. Ockwig, H.K. Chae, M. Eddaoudi, J. Kim, Nature 423 (2003) 705;
(c) E. Coronado, D. Gatteschi, J. Mater. Chem. 423 (2006) 2513.
[2] (a) L. Brammer, Chem. Soc. Rev. 33 (2004) 476;
(b) D. Bradshaw, J.B. Claridge, E.J. Cussen, T.J. Prior, M.J. Rosseinsky, Acc. Chem. Res. 38 (2005) 273;
(c) J.L.C. Rowsell, O.M. Yaghi, Angew. Chem. Int. Ed. 44 (2005) 4670.
[3] (a) S. Kitagawa, S. Noro, T. Nakamura, Chem. Commun. 45 (2006) 701;
(b) J.-Y. Zhang, C.-M. Liu, D.-Q. Zhang, S. Gao, D.-B. Zhu, CrystEngComm 9 (2007) 799;
(c) S.-Q. Zang, Y. Su, Y.-Z. Li, J.-G. Lin, X.-Y. Duan, Q.-J. Meng, S. Gao, CrystEngComm 11 (2009) 122.
[4] (a) C. Seward, J. Chan, D. Song, S.-N. Wang, Inorg. Chem. 42 (2003) 1112;
(b) S. Hu, A.-J. Zhou, Y.-H. Zhang, S. Ding, M.-L. Tong, Cryst. Growth. Des. 6 (2006) 2543;

- (c) J.-Q. Liu, Y.-Y. Wang, L.-F. Ma, G.-L. Wen, Q.-Z. Shi, S.R. Batten, D.M. Proserpio, CrystEngComm 10 (2008) 1123.

[5] N.W. Ockwig, O. Delgado-Friedrichs, M. O'Keeffe, O.M. Yaghi, Acc. Chem. Res. 38 (2005) 176.

[6] (a) H. Chun, D. Kim, D.N. Dybtsev, K. Kim, Angew. Chem. Int. Ed. 43 (2004) 971;
  (b) R.-Q. Zou, R.-Q. Zhong, M. Du, T. Kiyobayashi, Q. Xu, Chem. Commun. (2007) 2467.

[7] (a) B. Chen, M. Eddaoudi, T.M. Reineke, J.W. Kampf, M. O'Keeffe, O.M. Yaghi, J. Am. Chem. Soc. 122 (2000) 11559;
  (b) K. Biradha, M. Fujita, Angew. Chem. Int. Ed. 41 (2002) 3392;
  (c) M. Eddaoudi, J. Kim, N. Rosi, D. Vodak, J. Wachter, M. O'Keeffe, O.M. Yaghi, Science 295 (2002) 469.

[8] (a) N.R. Kelly, S. Goetz, S.R. Batten, P.E. Kruger, CrystEngComm 10 (2008) 68;
  (b) Y. Cui, M.-L. Cao, L.-F. Yang, Y.-L. Niu, B.-H. Ye, CrystEngComm 10 (2008) 1288;
  (c) J. Yang, J.-F. Ma, Y.-Y. Liu, S.R. Batten, CrystEngComm 11 (2009) 151.

[9] (a) X.-J. Li, R. Cao, Z.-G. Guo, W.-H. Bi, D.-Q. Yuan, Inorg. Chem. Commun. 9 (2006) 551;
  (b) H.-Q. Hao, J. Wang, W.-T. Liu, M.-L. Tong, CrystEngComm 10 (2008) 1449;
  (c) J. Lu, W.-H. Bi, F.-X. Xiao, S.R. Batten, R. Cao, Chem. Asian J. 3 (2008) 542.

[10] (a) M. O'Keeffe, M. Eddaoudi, H. Li, T. Reineke, O.M. Yaghi, J. Solid. State Chem. 152 (2000) 3;
  (b) R. Natarajan, G. Savitha, P. Dominiak, K. Wozniak, J.N. Moorthy, Angew. Chem. Int. Ed. 44 (2005) 2115;
  (c) M. Du, Z.-H. Zhang, L.-F. Tang, X.-G. Wang, X.-J. Zhao, S.R. Batten, Chem. Eur. J. 13 (2007) 2578.

[11] (a) R. Cao, J. Lu, S.R. Batten, CrystEngComm 10 (2008) 784;
  (b) Y.-Q. Lan, S.-L. Li, Y.-G. Li, Z.-M. Su, K.-Z. Shao, X.-L. Wang, CrystEngComm 10 (2008) 1129;
  (c) R. Heck, J. Bacsa, J.E. Warren, M.J. Rosseinsky, D. Bradshaw, CrystEngComm 10 (2008) 1687.

[12] (a) K.-W. Chi, C. Addicott, M.-E. Moon, H.J. Lee, S.C. Yoon, P.J. Stang, J. Org. Chem. 71 (2006) 6662;
  (b) R.-Q. Zhong, R.-Q. Zou, M. Du, L. Jiang, T. Yamada, G. Maruta, S. Takeda, Q. Xu, CrystEngComm 10 (2008) 605;
  (c) O.R. Evans, W. Lin, Chem. Mater. 13 (2001) 2705;
  (d) T.-B. Lu, R.L. Luck, Inorg. Chim. Acta 351 (2003) 345;
  (e) G. Ou, J. Gu, T. Lu, R.L. Luck, J. Mol. Struct. 740 (2005) 143;
  (f) M.-H. Zeng, M.-C. Wu, S.W. Ng, Acta Cryst. E62 (2006) m661;
  (g) R. Sekiya, S. Nishikiori, K. Ogura, Chem. Lett. 35 (2006) 614;
  (h) R. Sekiya, S. Nishikiori, K. Ogura, Inorg. Chem. 45 (2006) 9233.

[13] Synthesis. Complexes **1**–**4** were prepared by using a similar procedure as described below. To a DMF (5 mL) solution of 3,4-Hpybz (0.05 mmol) was added a CH_3OH (10 mL) solution of metal salt (0.10 mmol, $MnCl_2 \cdot 4H_2O$ for **1**, $Zn(NO_3)_2 \cdot 6H_2O$ for **2**, $Cd(NO_3)_2 \cdot 4H_2O$ for **3**, and $Pb(NO_3)_2$ for **4**). After stirring for ca. 30 min, the mixture was filtered and left to stand at room temperature. Colorless block (for **1**–**3**) or needle-shaped (for **4**) crystals were obtained by slow evaporation of the solvents for ca. two weeks. Yield: 43% for **1**, 51% for **2**, 39% for **3**, and 66% for **4**. Anal. Calcd for $C_{48}H_{34}Mn_2N_4O_9$ (**1**) (Mr=920.67): C, 62.62; H, 3.72; N, 6.09%; Found: C, 62.50; H, 3.64; N, 6.16%. IR (cm^{-1}): 3447b, 1619vs, 1556s, 1426s, 1398vs, 1328s, 1192m, 1101m, 1031m, 1006m, 817s, 780s, 754s, 705s, 643m, 473s. Anal. Calcd for $C_{48}H_{34}Zn_2N_4O_9$ (**2**) (Mr=941.57): C, 61.23; H, 3.64; N, 5.95%; Found: C, 61.30; H, 3.74; N, 5.86%. IR (cm^{-1}): 3421bs, 3224s, 1626s, 1607s, 1541s, 1378vs, 1194 m, 1134 m, 1069w, 1035m, 1007m, 865m, 817m, 779vs, 705s, 645m, 552m, 476m. Anal. Calcd for $C_{48}H_{34}Cd_2N_4O_9$ (**3**) (Mr=1035.61): C, 55.67; H, 3.31; N, 5.41%; Found: C, 55.76; H, 3.45; N, 5.32%. IR (cm^{-1}): 3428bs, 1612vs, 1558m, 1474w, 1428m, 1389vs, 1333m, 1192w, 1101w, 1031w, 1007m, 867 m, 816m, 779s, 704m, 641m, 535m, 466m. Anal. Calcd for $C_{24}H_{16}N_2O_4Pb$ (**4**) (Mr=603.58): C, 47.76; H, 2.67; N, 4.64%; Found: C, 47.86; H, 2.58; N, 4.56%. IR (cm^{-1}): 1594s, 1548s, 1432w, 1353vs, 1195m, 1130m, 1003w, 867w, 843m, 778s, 703m, 667w, 622w, 551w, 528w, 474 m.

[14] Crystallographic data for **1**: $C_{48}H_{34}Mn_2N_4O_9$, M=920.67, $0.18 \times 0.14 \times 0.13$ mm^3, monoclinic, space group $C2/c$, a=11.982(3), b=15.316(4), c=21.926(5) Å, β=95.607(4)°, V=4005(2) Å^3, Z=4, D_c=1.527 g/cm^3, F(000)=1888, GOF=1.141, μ=0.698 mm^{-1}, R=0.0670, and wR=0.1607. Crystallographic data for **2**: $C_{48}H_{34}Zn_2N_4O_9$, M=941.57, $0.24 \times 0.20 \times 0.18$ mm^3, monoclinic, space group $C2/c$, a=11.863(2), b=15.487(3), c=21.635(5) Å, β=94.938(4)°, V=3960(1) Å^3, Z=4, D_c=1.579 g/cm^3, F(000)=1928, GOF=1.048, μ=1.279 mm^{-1}, R=0.0274, and wR=0.0661. Crystallographic data for **3**: $C_{48}H_{34}Cd_2N_4O_9$, M=1035.61, $0.24 \times 0.22 \times 0.18$ mm^3, monoclinic, space group $C2/c$, a=12.022(3), b=15.243(3), c=22.350(5) Å, β=95.942(5)°, V=4074(2) Å^3, Z=4, D_c=1.689 g/cm^3, F(000)=2072, GOF=1.017, μ=1.110 mm^{-1}, R=0.0242, and wR=0.0515. Crystallographic data for **4**: $C_{24}H_{16}N_2O_4Pb$, M=603.58, $0.28 \times 0.14 \times 0.12$ mm^3, orthorhombic, space group $Pccn$, a=10.704(2), b=21.357(4), c=8.635(2) Å, V=1974.0(6) Å^3, Z=4, D_c=2.031 g/cm^3, F(000)=1152, GOF=1.013, μ=8.583 mm^{-1}, R=0.0160, and wR=0.0353.

[15] L. Shimoni-Livny, J.P. Glusker, C.W. Bock, Inorg. Chem. 37 (1998) 1853.

[16] (a) M.H. Jack, M. Saeed, A.S. Ali, Inorg. Chem. 43 (2004) 1810;
  (b) Y.-Q. Xu, D.-Q. Yuan, L. Han, E. Ma, M.-Y. Wu, Z.-Z. Lin, M.-C. Hong, Eur. J. Inorg. Chem. (2005) 2054;
  (c) X. Li, R. Cao, Z. Guo, J. Lu, Chem. Commun. (2006) 1938.

[17] (a) M. Du, H. Cai, X.-J. Zhao, Inorg. Chim. Acta 359 (2006) 673;
  (b) J. Yang, G.-D. Li, J.-J. Cao, Q. Yue, G.-H. Li, J.-S. Chen, Chem. Eur. J. 13 (2007) 3248;
  (c) A. Pellissier, Y. Bretonnière, N. Chatterton, J. Pécaut, P. Delangle, M. Mazzanti, Inorg. Chem. 46 (2007) 3714.

[18] For the three-letter net codes, see Ref. [5] and the associated website 〈http://rcsr.anu.edu.au/〉.

[19] V.A. Blatov, Acta Cryst. A 63 (2007) 329.

[20] The ideal space group (true symmetry) for this network is $P4_2/ncm$.